Available online at www.sciencedirect.com
SCIENCE DIRECT®
Journal of Sound and Vibration 264 (2003) 689–706
JOURNAL OF SOUND AND VIBRATION
www.elsevier.com/locate/jsvi

A study of the transition to instability in a Rijke tube with axial temperature gradient

K.I. Matveev, F.E.C. Culick*

Jet Propulsion Center, California Institute of Technology, MC 205-45 Pasadena, CA 91125, USA

Received 16 January 2002; accepted 10 July 2002

Abstract

A horizontal Rijke tube with an electric heat source is a system convenient for studying the fundamental principles of thermoacoustic instabilities both experimentally and theoretically. Given the long history of the device, there is a surprising lack of accurate data defining its behavior. In this work, the main system parameters are varied in a quasi-steady fashion in order to find stability boundaries accurately. The chief purposes of this study are to obtain precise values of the system parameters at the transition to instability with specified uncertainties and to determine how well the experimental results can be explained with existing theory. Measurement errors are reported, and the influence of experimental procedures on the results is discussed. A form of hysteresis effect at stability boundaries has been observed. Mathematical modelling is based on a thermal analysis determining the temperature of the heater and the temperature field in the air inside the tube, which, consequently, affects acoustical mode shapes. Solutions of the linearized wave equation for a non-uniform medium, including losses and a heat source term, determine the stability properties of the eigen modes. Calculated results are compared with experimental data and with results of the modelling based on the common assumption of a constant temperature in the tube. The mathematical model developed here can be applied to designing thermal devices with low Mach number flows, where thermoacoustic issue is a concern.

1. Introduction

Thermoacoustic instabilities refer to the appearance of pressure oscillations inside chambers coupled with an unsteady heat release. This effect is important in technical applications such as rocket motors [1], low-pollutant lean flames [2], and thermoacoustic engines [3]. Rayleigh's criterion [4] states that acoustic oscillations are encouraged when heat is added to the air at the

*Corresponding author. Tel.: +1-626-395-4783; fax: +1-626-395-8469.
E-mail addresses: matveev@caltech.edu (K.I. Matveev), fecfly@caltech.edu (F.E.C. Culick).

0022-460X/03/$ - see front matter
doi:10.1016/S0022-460X(02)01217-8

moments of condensation or extracted at the moments of rarefaction; and oscillations are discouraged if heat is abstracted during condensation or given at rarefaction. That means that the necessary condition for thermoacoustic instability is the existence of an unsteady heat release component that fluctuates in phase with pressure oscillations. Rayleigh's criterion can be conveniently expressed via transformation of thermal energy into acoustic energy during one cycle of oscillation [5]:

$$\Delta E = \frac{(\gamma - 1)}{p_0 \gamma} \int \mathrm{d}V \int_t^{t+T} p' \dot{Q}' \, \mathrm{d}\tau, \tag{1}$$

where p' and $\dot{Q}'$ are the pressure and heat release fluctuations, and T is the cycle period. If this energy input exceeds acoustic losses, then the system becomes unstable.

Since thermoacoustic instability is a complex phenomenon, some simplified models must be used to understand its nature. A Rijke tube is a convenient system for studying thermoacoustic instabilities both experimentally and theoretically. The original Rijke tube [6] consisted of a vertical pipe with a gauze, located in the lower half of the tube and heated by a flame (Fig. 1). A mean flow in the tube appears due to natural convection. For sufficiently high temperature of the gauze, a high-intensity tone is generated. A simple explanation of sound appearance in a Rijke tube, using Eq. (1), is given in Appendix A.

Despite its simplicity, a vertical Rijke tube does not permit independent variation of the mean flow and the power supplied to a gauze. A horizontally located Rijke with a mean flow, provided by a blower, and an air-permeable gauze, heated by electric current, overcomes this deficiency. Another advantage of an electric Rijke tube is the possibility for precise control of the main system parameters in wide ranges: heater location, air flow rate, and heat power released. In our experiments, this type of a Rijke tube is employed. For a certain range of the main system parameters, the tube produces a tonal sound with frequencies close to the natural frequencies of the system.

Previous experiments on Rijke tube devices were reviewed by Raun et al. [7]. There are articles [8–10] that contain extensive information on stability boundaries, limit cycle amplitudes and frequencies of excited modes for sets of basic system parameters. However, little information has been given about the experimental procedures, in particular how the controllable parameters were

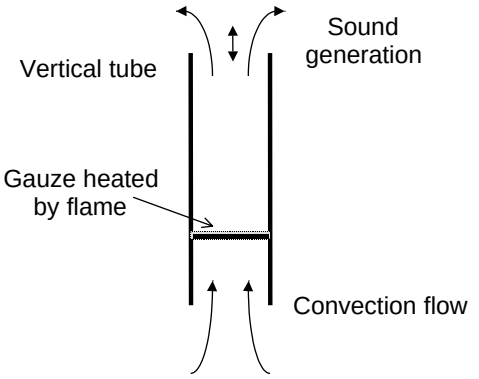

Fig. 1. Vertical Rijke tube.

varied. Experimental errors have not been reported in the previous works and temperature measurements have been rarely accomplished. The main exception is the paper by Finlinson et al. [11] on the Rijke tube burner. All these factors strongly affect the observed transition to instability.

Mathematical models for transition to instability in a Rijke tube were reviewed by Raun et al. [7]. A significant deficiency in the most previous works is the absence of a thermal analysis, which determines the temperature distribution in a tube. Mode shapes and matching conditions on the heater, defining transition to instability, are very dependent on the non-uniform temperature field. Raun and Beckstead [12] developed an interpolating model for determining the average temperature profile based on the simplified energy equation and temperature measurements at certain points in the burner. Though less critical due to its small value, the heater impedance is usually neglected. Heat transfer characteristics of the heater are of great importance for stability properties. For some limiting values of the system parameters, analytical estimations can be obtained [13–15]; for flow conditions unsuitable for theoretical analysis, CFD is used [16].

At the present time, the qualitative reasons for Rijke oscillations are well understood with the remaining uncertainty in the unsteady heat transfer at the heater. However, there is lack of both the experiments providing accurate data and the models capable of accurately predicting the transition to instability in thermoacoustic devices, and this paper attempts to advance in that direction. A primary objective of this and companion works is to provide accurate experimental data for comparison with comprehensive analysis of both linear and non-linear behavior. Success will provide basic understanding of the simplest example of thermoacoustic instabilities.

This paper is the development of the study [17] initiated by the authors on a Rijke tube at the Jet Propulsion Center, Caltech. Experimental and data acquisition systems are described in the following section. Experimental strategy, samples of time-resolved measurements, and stability boundaries for three heater locations with the associated errors are reported. The heat transfer model developed in Ref. [17] serves as the basis for determining the acoustical modes and their stability properties from a wave equation for a particular set of system parameters. Stability boundaries are calculated and compared with those obtained experimentally and with those computed under the assumption of the constant temperature in the tube. The difference between results of the two theories is significant.

2. Experimental setup

The structure of the experimental apparatus is shown in Fig. 2. The important elements of the system are described in this section; more detailed information can be found in Ref. [18]. The horizontally placed Rijke tube is a square aluminum tube of $9.5 \times 9.5\,\mathrm{cm}^2$ cross-section and length 1.0 m. The thickness of tube walls is 3 mm. Mean air flow is provided by a blower, which sucks air in the tube. The usage of a fan allows us to control a major system parameter, the mean flow rate, precisely and independently of the thermal power release, which is also regulated. If the tube were kept vertically orientated, as in the original version by Rijke, then, first, it would be necessary to take into account a mean flow component caused by natural convection in the stability analysis, and secondly, it would be difficult to provide low rates of mean flow at high levels of power. To exclude the influence of natural convection on a mean flow rate, the horizontal orientation of the

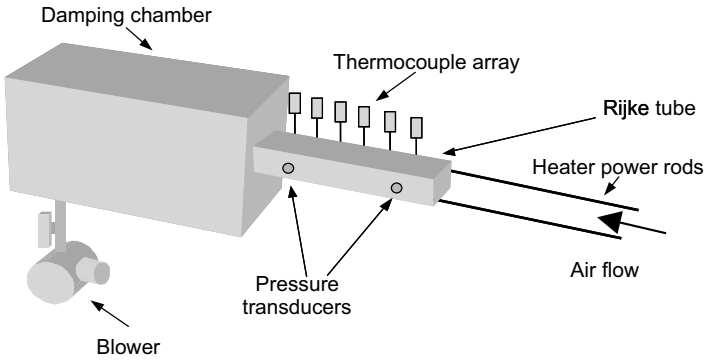

Fig. 2. Experimental setup of the Rijke tube.

Rijke tube has been implemented. A damping chamber, located between the tube and the blower, is intended to prevent influence on the blower from tube acoustics. The chamber dimensions are $46 \times 46 \times 120\,\mathrm{cm}^3$; its internal surface is covered by a $1/2''$ pile carpet on a $1/8''$ felt.

Since the major mystery about Rijke oscillations is associated with a heat transfer at the heater, it is desirable to select a heater with the heat transfer process that can be analytically modelled as precisely as possible. This suggests an array of parallel cylinders, located far from each other. In order to consider a heater to be infinitely thin in mathematical modelling (it would permit to apply jump conditions), the cylinder diameter must be small, hence, a set of wires could be used. To measure stability properties of a Rijke tube in wide ranges of system parameters, a heater should also repeatedly withstand high temperatures for long time intervals and be able to release large amounts of thermal power (over 1 kW in our system) without changes in geometry. Another desirable property is the ability to heat the air flow uniformly over a tube cross-section. A square-weave 40-mesh made from nichrome is a suitable trade-off between these requirements. It has proved to be a reliable heating element, and the heat transfer resembles that from cylinders, accounting for a flow blockage effect. A wire diameter in this grid is $0.01''$. The gauze is brazed to two strips of copper, which are suspended on a square frame made from macor (machinable glass ceramic) in order to eliminate electric and reduce thermal contact with tube walls. The lay of the screen is parallel to the direction of electric current flow. Two copper rods with diameter $0.25''$, welded directly to the copper strips on the heater, connect the heater to the power source. The power source consists of two TCR-20T250 power supplies, each capable of producing 500 A of current. The power supplies are load balanced and operate in parallel. The actual power supplied is dependent on the resistance of the nichrome grid, which changes with temperature. The power supplies are computer controlled using a software-implemented controller to stabilize the output power, although fluctuations on the order of $\pm 1\%$ do occur with a frequency 60 Hz. The location of the heater can be easily changed within the tube.

The mean air flow through the Rijke tube is provided by a GAST R1102 blower, operating at 3450 r.p.m. with a maximum throughput of $0.0127\,\mathrm{m}^3/\mathrm{s}$ at standard atmospheric conditions. The blower is operated at full capacity with a $2''$ by-pass ball valve controlling the amount of air drawn through the damping chamber, or from the atmosphere. A large plastic shroud (not pictured) is placed above the entrance to the Rijke tube to minimize the effects of external air currents on the

system. The flow rate is measured using a laminar flow element (Meriam 50MW20) and a differential pressure transducer (Honeywell Microswitch). This measurement takes place between the damping chamber and the blower. A thermocouple, located upstream of the laminar flow element, is used to correct for air density and viscosity to produce the total air mass flow rate.

Pressure transducers used in this experiment must be able to provide accurate measurements in a hot environment. The transducers used were PCB model 112A04, coupled with a 422D11 charge amplifier and a 482A20 signal conditioner. Charge-mode piezoelectric transducers were used, since the majority of the electronics is located in a separate charge amplifier, increasing the operating temperature range while retaining relatively high sensitivities. The two pressure transducers are flush mounted in the tube at positions $x/L = 0.15$ and 0.80.

In determination of stability boundaries, an array of 15 type K thermocouples is suspended from the top of the tube to the centerline. An additional thermocouple is located just before the laminar flow element that measures the mean flow through the tube. The spacing was selected to place more thermocouples nearer to the heat source, as well as to allow the heater to be located at key locations without interfering with the thermocouples. For validating the thermal modelling, some thermocouples were used at the exit and entrance cross-sections for determination of averaged temperature in those sections. Since the thermocouples have a relatively large time constant, they are multiplexed and sampled at 2 Hz. It is not possible for thermocouples to respond quickly enough at the acoustic time scales required in the experiment. They are used solely for time-averaged temperature measurements.

In order to provide accurate measurements of the acoustic pressures and other relevant parameters in the Rijke tube, a fast sampling system is required. The data acquisition system is based on a Pentium III 700 MHz computer. A Computer Boards' CIO-DAS1602/12 (12 bit) data acquisition board is installed in the machine, using the Sparrow program [19] as the software interface. An EXP-16 expansion board accommodates the 16 thermocouples in a multiplexed array and also provides cold junction compensation. The DAS1602/12 is operated in single-ended mode, giving a total of up to 16 analog input channels. It also contains two analog output channels, one of which is used to control the power supplies. In this configuration, data could be acquired in short bursts at over 8000 Hz, and for extended periods of time streaming to the hard drive at over 4000 Hz. For this Rijke tube, the frequencies of the primary excited modes are approximately 180 and 360 Hz. These frequencies and the waveforms are easily captured by the data acquisition system.

3. Experimental procedure and results

In the experiments reported here, there are three basic parameters that can be controlled: heater position, air flow rate, and power supplied to the heater. Since the first two parameters are changed mechanically, they were fixed in the individual experimental runs, and power was varied through the computer interface of the control system. Stability boundaries were determined for three heater locations: 1/4, 1/8 and 5/8 of the tube length; the origin of the tube is taken to be at the open upstream end. For each heater position, a set of mass flow rate values was selected to cover the range when transition to instability is possible. Then the power was varied, beginning from zero, in order to find a critical power when transition to instability occurs.

Following a change of power, the temperature field in the tube slowly responds. This unsteadiness as well as finite power increments can lead to initiation of the instability at a lower power than it would be in the system with steady temperature distribution corresponding to a certain power level. It was observed in the experiment that the critical power obtained with large step variations of power level may significantly differ from the critical power obtained at small steps.

To avoid this early initiation and to give results convenient for mathematical modelling, a quasi-steady procedure for power variation was established. First, a settling time was imposed between power changes; during that time a steady temperature field was reached in the system. This time (of the order of a few minutes) was determined experimentally for different system configurations. Second, to obtain a critical power accurately, power increments should be as small as possible, but this could lead to an unreasonable increase in the duration of the experiment. An iterative method with reduction of a power step was implemented. Initially, large steps (50 W) were used for approximately locating the transition to instability; then this boundary was approached from below with smaller power increments, so that the accuracy in locating this boundary was improved. A step in power variation was successively reduced until a converged value of the critical power was obtained; the minimally possible step corresponds to the intrinsic power oscillation of order of 1%.

Since transition from the stable to the unstable state does not coincide exactly with the reverse transition, another critical power was also determined, corresponding to the transition from the unstable to the stable state. After excitation of the instability, several power increments were made in order to move from the transition point, then power was decreased, using the same (small) steps and settling time, until a stable state was achieved. Almost always, the critical power in the backward direction was smaller than in the forward one. The presence of a large gap between the two critical powers may imply hysteresis of the stability boundary. However, that is not always the case: in the unstable regime, temperatures in the system increase due to acoustically enhanced heat transfer, leading to a change in the mass flow rate. Hence the forward and backward paths may correspond to different mass flow rates. Also, errors in the mass flow rate and power must be taken into account, since they can overlap the gap between those two critical powers. Thus, only by plotting the critical points with error bars on the power–mass flow rate diagram is it possible to determine whether hysteresis is present.

For each power step, a time-resolved measurement of the pressure (at two points), temperature (at 15 points), a mass flow rate and a supplied power were recorded. The examples of pressure fluctuations in time (cold section transducer) and the temperature profile along the tube centerline are given in Fig. 3 for an unstable case (heater position is 1/4 of the tube). Typically, the pressure oscillation is quite regular, showing some evidence of harmonic content with only small cycle-to-cycle variations. Temperature records demonstrate the jump at the heater location and non-uniform temperature profiles in both cold and hot sections of the tube.

Examples of the experimental runs for determining transition to instability are shown in Fig. 4 for moderate and high mass flow rates; the noise component has been eliminated. In the second case shown in Fig. 4(b), a significant gap between the critical powers on the forward and backward paths is present; this difference is referred as hysteresis: two different states (stable and unstable) can exist at the same values of the system parameters. The presence of a particular state depends on the history of the parameter variations.

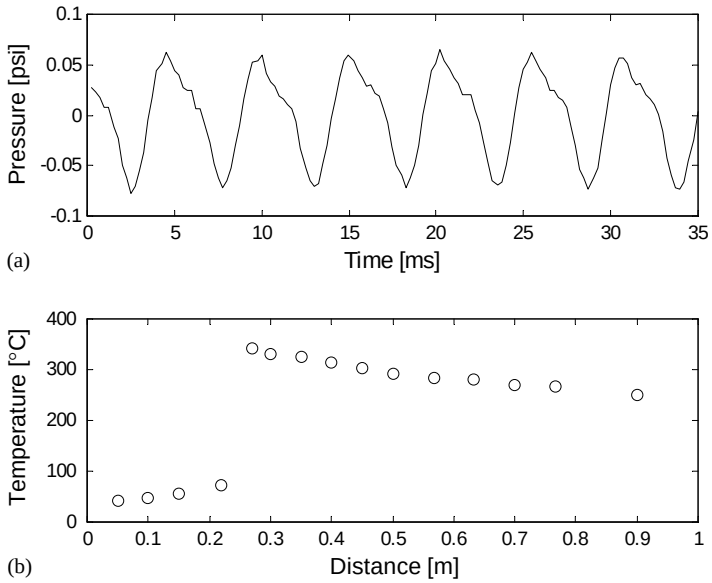

Fig. 3. (a) Records of pressure by the cold section transducer; and (b) measured centerline temperature. Power 1073 W; mass flow rate 3.18 g/s.

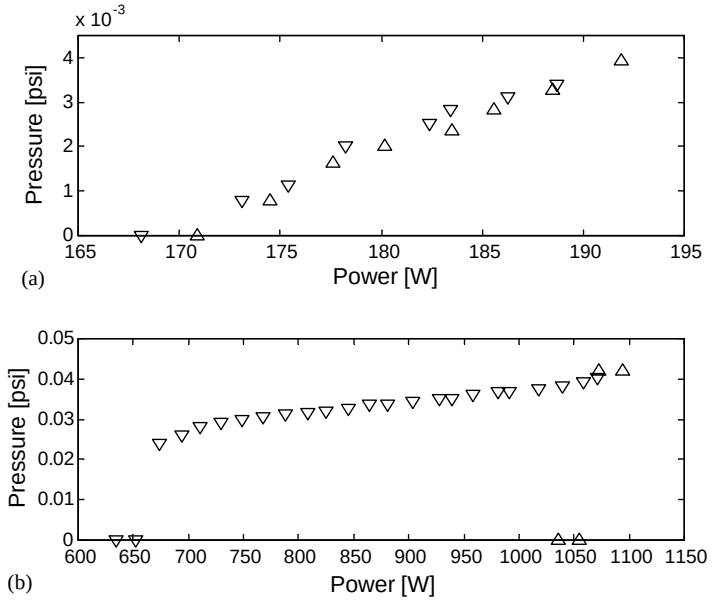

Fig. 4. r.m.s. of pressure oscillations for mass flow rates: (a) 1.05 g/s; (b) 3.15 g/s (Δ = power increase; ∇ = power decrease).

Fig. 5 shows the stability boundaries as functions of power and mass flow rate for different heater locations. Critical values are given with experimental error bars. The mode with frequency around 180 Hz is responsible for the transition to instability in cases (a) and (b), although in the

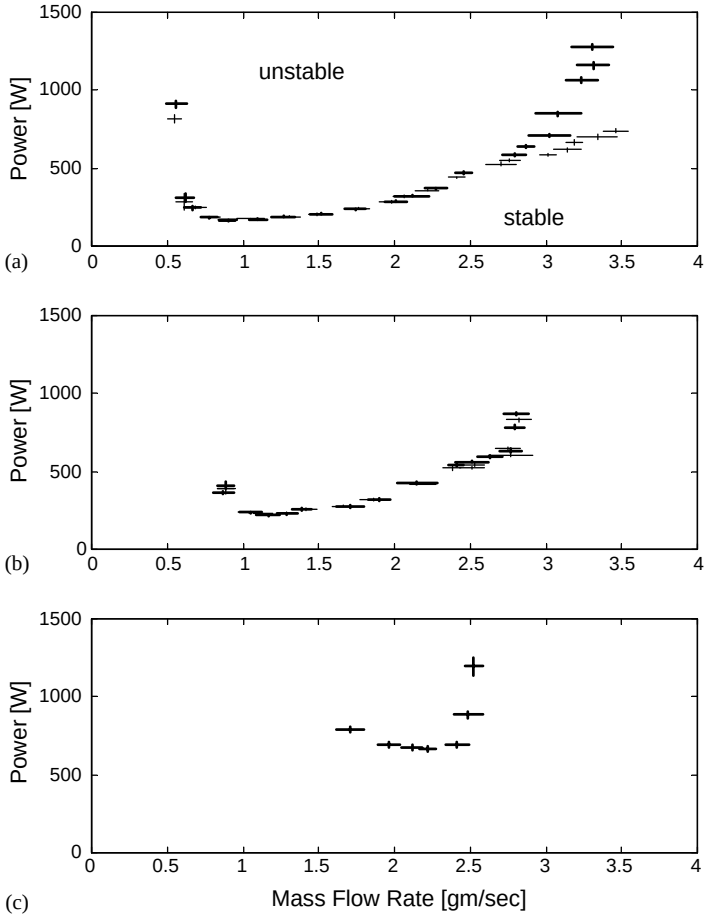

Fig. 5. Transition to instability for heater positions: (a) 1/4; (b) 1/8; and (c) 5/8 of the tube length. Bold lines correspond to power increase, light lines to power decrease.

unstable regime other harmonics are also present. Note that in the first case significant hysteresis in the transition between stable and unstable regimes is present at high mass flow rates. The general shape of the stability curves is in agreement with previous investigations on Rijke tubes.

When a heater is located in the downstream half of the tube as in case (c), the first mode cannot be excited due to unfavorable correlation between pressure and heat release fluctuations, as shown in Appendix A. The initial system configuration made losses for higher modes so large, that they also were not producible in the accessible range of power. To reduce damping, the back wall of the chamber, initially covered by a carpet, was made rigid. As a result, the second mode with frequency around 360 Hz became excitable. When power was increased further above the stability boundary, sound disappeared at some point, so that no stability boundary is presented for power decrease.

Only experimentally determined stability boundaries, and the linear analysis, intended to locate them, are the subjects of this paper. Within this study, we recorded only steady responses at the

steady temperature fields; growth rates of the excited modes at transition through the stability boundary, corresponding to transient processes, are not reported here. Hysteretic behavior, excited modes in unstable regimes, their frequencies and limit-cycle amplitudes are defined by non-linear properties of the system. Those results are not covered here but will be the subject of a later publication.

4. Thermal analysis

In previous investigations of the Rijke tube, the temperature was usually assumed to be constant in cold and hot sections of the tube. However, transition to instability is dependent on the eigen mode shapes, which are sensitive to the temperature field; so more attention should be paid to the analysis of global heat transfer aimed at finding the temperature distribution and heat flux along the tube. Also, the temperature of the heater is an important parameter determining transition to instability; it can be accurately found only from a complete heat transfer model. Thermal analysis is, of course, important for any thermal device independently of the presence of thermoacoustic problems. The temperature profile recorded along a tube centerline (Fig. 3(b)) exhibits significant non-uniformity and shows the necessity for performing thermal modelling to determine the temperature profile.

A heat transfer model constructed by the authors in Ref. [17] is applied in this study. Equations for the heat balance are formed for the grid and for the elements of the tube, rods and air inside the tube as functions of the horizontal co-ordinate. The scheme of the system for the thermal analysis is shown in Fig. 6. Appropriate empirical correlations for heat transfer rates are applied for heat exchange between structural elements. All types of heat transfer are taken into account: both types of convection, heat conduction and thermal radiation. A natural convection from the grid to the air flow inside the tube is much weaker than a forced convection for the ranges of parameter variation typical in our system; hence, it is assumed that a heat transfer from the heater to the air flow is of a forced convective type only. The flow is assumed to be steady in thermal modelling aimed at finding a steady temperature field. Substituting heat transfer correlations into heat balance equations, a non-linear system of equations for temperature field is obtained; the system is solved numerically applying an iterative procedure.

One example of the experimental results for the temperature field and the calculated temperature profiles are shown in Fig. 7. For illustrative purposes, the temperature of the air flow at the centerline is shown. Note that the centerline temperature can significantly deviate from the

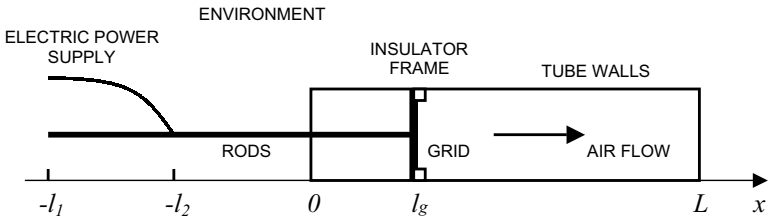

Fig. 6. Structural model for thermal analysis.

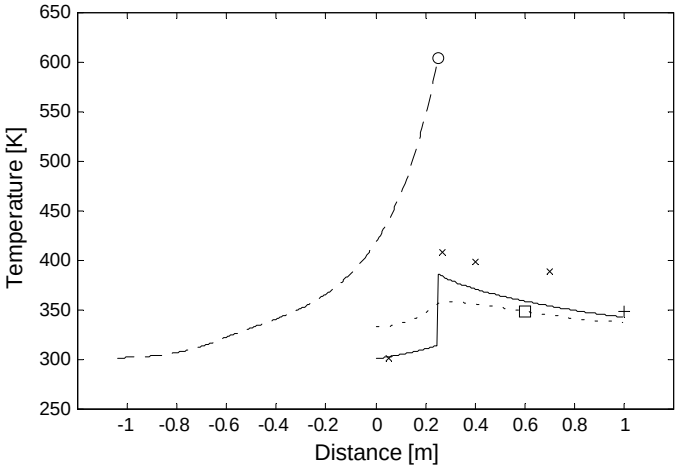

Fig. 7. Calculated temperatures of the air flow (—), tube walls (· · ·), copper rods (- - -), and the grid (○). Measured temperatures: □ mean temperature of the tube wall, + mean temperature at the tube exit; × air flow centerline temperature. Power 383 W; mass flow rate 3.76 g/s.

mean cross-section temperature; there is a hot core on the centerline of the flow since the grid heats incident air more effectively at the centerline than at the boundaries and the heat exchange with the tube walls affects mostly air layers adjacent to the walls. A series of temperature measurements was carried out to check the validity of the thermal model over a range of system parameters. All experimental data corresponding to low and moderate power levels coincide with the calculated temperature within experimental error; in high-power regimes, deviation of the calculated from experimental results slightly exceeds experimental error. Thus, this mathematical model is able to predict temperature profiles reliably for the basic system parameters in the range of the primary interest, and gives an approximate estimation for extreme regimes.

5. Stability analysis

In our model, the investigation of transition to instability is based on the one-dimensional linear wave equation for the pressure fluctuations p' in the medium having non-uniform temperature with volumetric source intensity Ω and heat addition $\dot{Q}'$ [1,20]:

$$\frac{\partial^2 p'}{\partial t^2} - a^2\frac{\partial^2 p'}{\partial x^2} + \frac{a^2}{\rho_0}\frac{\partial \rho_0}{\partial x}\frac{\partial p'}{\partial x} = (\gamma - 1)\frac{\partial \dot{Q}'}{\partial t} + \rho_0 a^2 \frac{\partial \Omega}{\partial t}. \tag{2}$$

The sound velocity a and mean gas density ρ_0 are calculated for an ideal gas; subscript 0 stands for the values averaged in time and dependent on the horizontal co-ordinate only. The Mach number in our system is less than 10^{-3}, so that its effect on acoustics appears to be much smaller than the influence from the forcing terms in Eq. (2); hence, the mean flow is ignored in the stability analysis. The volumetric source intensity Ω in the wave equation, responsible for boundary layer losses, is related to the pressure perturbation by a standard expression available in Ref. [20]. The

solution for the wave equation is assumed to have the form

$$p'(x,t) = e^{\sigma t}\psi(x), \tag{3}$$

where σ is a complex number, and $\psi(x)$ is the complex-valued mode shape. Substituting Eq. (3) into Eq. (2) and applying the boundary conditions at the tube ends and matching conditions at the heating element, which is assumed to have a negligible horizontal dimension, the problem is closed. Each non-trivial solution corresponds to a certain eigenvalue $\sigma = \alpha + i\omega$; its real part α is the growth rate and the imaginary part ω is the frequency of the appropriate acoustical mode.

The dominant component of the unsteady heat addition in the system is the heat released by the grid. We make use of the matching conditions at the grid developed by Merk [13] for the upstream and downstream velocity perturbations in the case of the low Mach number,

$$u'_+ = \frac{c_{p-}}{c_{p+}}\left(1 + \left(\frac{c_{p+}T_+}{c_{p-}T_-} - 1\right)Tr_{Q,u}\right)u'_-, \tag{4}$$

where $Tr_{Q,u}$ is a transfer function between reduced velocity and heat release fluctuations, c_p is the heat capacity. Subscripts $+$ and $-$ stand for downstream and upstream sides. The transfer function, dependent on the mean flow velocity, frequency and fluid properties, is defined by the formula

$$\frac{\dot{Q}'}{\dot{Q}_0} = Tr_{Q,u}\frac{u'_-}{u_{0-}}. \tag{5}$$

The heat transfer function is the most important issue in the modelling of thermoacoustic instability. An extensive search of the literature has been carried out in order to find information about this function. Most suitable for our system are the results reported by Kwon and Lee [16] for the heat transfer of a cylinder in superimposed oscillating and steady flows. Employing the finite difference method, they calculated the time-dependent heat transfer response of the cylinder to the velocity fluctuations by treating the flow as incompressible and two-dimensional. In our system, the flow is in the intermediate regime when the Oseen approximation is already invalid and a boundary layer is not yet formed. The results in Ref. [16] cover most of this range.

It was shown in Ref. [16] that thermoacoustic power generation is most effective when the dimensionless mean flow velocity $u_0/\sqrt{\omega\kappa}$ and the wire radius $r\sqrt{\omega/\kappa}$ are around unity, meaning that at low and high mass flow rates it is more difficult to initiate instability than in some intermediate regime. The amplitude of the dimensionless velocity fluctuation $u'/\sqrt{\omega\kappa}$ was equal to unity (κ is a thermal diffusivity). At low flow rates, the assumption of small oscillating velocity with respect to the mean flow velocity was not strictly met; this can be a source of significant errors. Since no information is available in the literature for the transfer function in that range, we use the results reported in Ref. [16], keeping in mind the possible inaccuracy at low flow rates. The normalized unsteady heat release was described in Ref. [16] in the form of parametric plots for the absolute value and for the phase shift with respect to the velocity fluctuation. In our modelling, those functions are tabulated and transformed into the transfer function. For a particular system state, its value is found by interpolation. The heating element in our system is a grid composed of cylinders; in order to use the reported data, the effective velocity of the incoming flow is modified using a blockage factor. Information available in Ref. [16] does not cover the entire region of system parameter variations; the transfer function has to be extrapolated to the range of high

mass flow rates. Thus, the transfer function is probably not accurate at both low and high mass flow rates.

From the momentum equation, it can be shown that the acoustical velocity is related to the pressure perturbation as $u' = \mathrm{i}p'_x/\omega\rho_0$. Pressure perturbations just upstream and downstream of the gauze are related through the impedance condition [21]

$$p'_+ - p'_- = Z_g u'_p, \tag{6}$$

where u'_p is the area-averaged perforate velocity. Estimated for our system, Z_g appeared to be very small. At the tube ends, the pressure and velocity perturbations are related by

$$p' = Zu'. \tag{7}$$

One of the tube ends is unflanged and open, so that the corresponding impedance for the modes with wavelength much greater than the tube width is [22]

$$Z_1 = -\frac{\rho\omega^2 R^2}{4a} - \mathrm{i}\rho\omega l_{oe}, \tag{8}$$

where the equivalent tube radius is related to the side of a square section as $R = D_t/\sqrt{\pi}$ and the open end correction is $l_{oe} \approx 0.61R$. The other tube end is connected to the damping chamber. The impedance at this end Z_2 can be expressed in terms of the impedance of the chamber Z_3 and the end correction for such a junction [23]:

$$Z_2 = \frac{D_t}{D_c} Z_3 + \mathrm{i}\rho\omega l_{tc}, \tag{9}$$

where l_{tc} has been tabulated in Ref. [24]. The impedance Z_3 prescribed by the chamber at the entrance from the tube is expressed in terms of the chamber attenuation and the load at the downstream end:

$$Z_3 = \rho a \frac{Z_4 \cosh(\varepsilon L_c) + \rho a \sinh(\varepsilon L_c)}{Z_4 \sinh(\varepsilon L_c) + \rho a \cosh(\varepsilon L_c)}, \tag{10}$$

where ε is the attenuation coefficient [23], L_c is the chamber length, and Z_4 is found from the absorption coefficient data for the carpet [25], which covers the walls in the damping chamber.

The procedure for finding the mode shape and a corresponding eigenvalue is similar to that described in Ref. [12]. Substitution of the pressure perturbation (3) into wave equation (2) produces an ordinary differential equation for the mode shape with unknown parameter σ. The value of σ is calculated iteratively by applying Newton's method to match the impedances on the downstream side of the tube. If, for a given set of system parameters, the growth rate of one of the modes is positive, then the system is unstable.

The search for a stability boundary is similar to the experimental sequence: for a fixed heater location and mass flow rate, power is increased in a step fashion, starting from a low value, until an unstable state is discovered; then the step size is reduced to find the exact critical power corresponding to zero growth rate. At each set of the system parameters, the temperature field has to be recalculated. Computed in this way, critical power values are compared in Fig. 8 with the experimentally obtained stability boundaries corresponding to the power increase. This way of varying the power was chosen because the temperature distribution in this case was formed in the

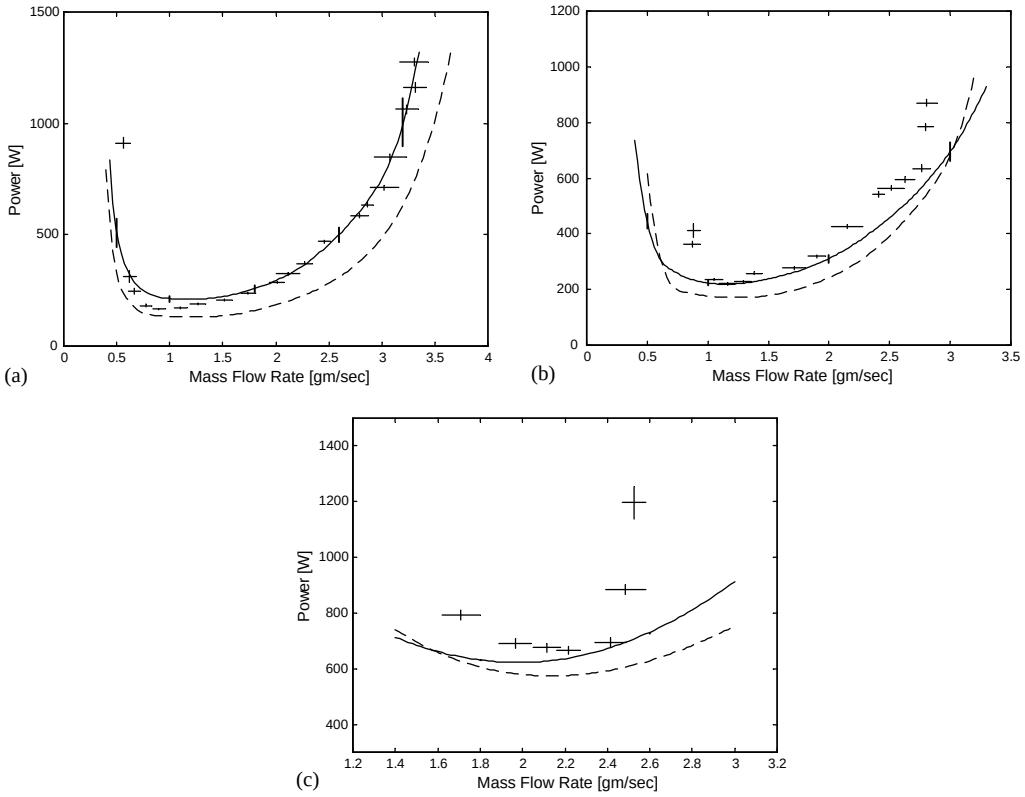

Fig. 8. Comparison of the experimental (+) and calculated (—) results for transition to instability. Solid lines correspond to the model incorporating spatial temperature variations; dashed lines to the model assuming uniform temperature in the tube. Bold vertical bars illustrate variation of the calculated stability boundary with respect to $\pm 20\%$ uncertainty in impedance Z_3. Heater position: (a) 1/4; (b) 1/8; and (c) 5/8 of the tube length from the upstream end.

situation when no oscillations were present, similar to the mathematical modelling. The critical power values found experimentally for the transition from the unstable to the stable state correspond to the higher temperatures in the system due to enhanced heat transfer in oscillating flow; hence, modified mode shapes and frequencies might affect the location of the stability boundary on the backward path. This is a possible reason for the hysteresis found in the experiments.

The agreement between the experimental data and the results obtained by the model incorporating temperature variations is satisfactory, taking into account the assumptions of one-dimensional flow and those used in computation of the heat transfer function. The highest deviations of the calculated stability curves are observed at low and high flow rates, where the transfer function is not accurate. In the third case (Fig. 8(c)), the discrepancy is greater, probably because a higher mode is responsible for instability in this case, and the acoustic assumption about the chamber narrowness is not strictly fulfilled. The highest uncertainty in the system parameters, used in modelling, is associated with the chamber impedance Z_3. No experimental attempts have

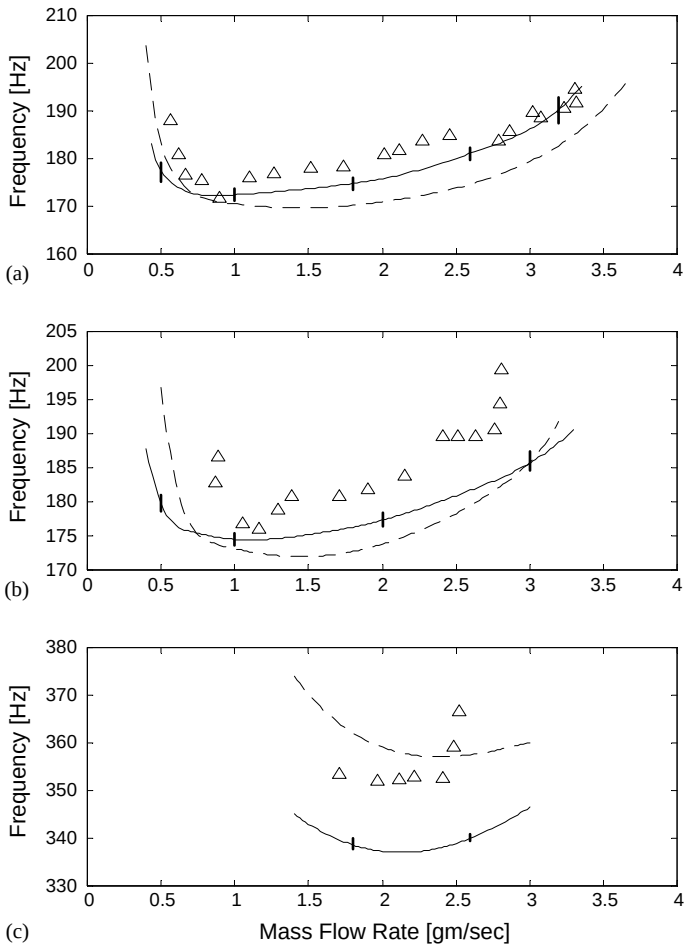

Fig. 9. Calculated dependence of critical frequencies on mass flow rates: solid lines correspond to the model incorporating spatial temperature variations; dashed lines to the model assuming uniform temperature in the tube. Bold vertical bars illustrate the variation of the critical frequency with respect to $\pm 20\%$ uncertainty in impedance Z_3. Δ is the measured dominant frequency after the transition to instability. Heater position: (a) 1/4; (b) 1/8; and (c) 5/8 of the tube length from the upstream end.

been made to measure this quantity. Vertical error bars, reflecting variation of the modelled stability boundary based on $\pm 20\%$ uncertainty in Z_3, are plotted in Fig. 8. In case (c), chamber properties are modified ($Z_4 = \infty$), that make the error bars very small.

In previous investigations, the models aimed at finding stability boundaries in Rijke tubes commonly used the assumption of a constant temperature in the entire tube [16,20,26]. To check how well this approximation works for our system, the transition to instability has been modelled within that assumption. The temperature of the air flow in this case is found by averaging temperature distribution along the tube. The temperature of the heater and the heat transfer rate from the grid to the air flow are taken from thermal analysis. As shown in Ref. [27], the critical power, corresponding to the transition to instability in this model, can be approximately

expressed by the formula

$$P^*_{cr} = -m\frac{\omega^2 D_t^3 + 2\pi aDt\,\mathrm{Re}(Z_2)/\rho + 4\sqrt{2}\pi aL\sqrt{\omega}\left(\sqrt{v} + (\gamma-1)\sqrt{\kappa}\right)}{2(\gamma-1)\pi D\sin(2l\omega/a)\mathrm{Im}(Tr)}, \tag{11}$$

where P^* is the fraction of the electric power supplied to the grid that is transferred to the air flow via forced convection (the remained portion of the supplied power leaves the grid in form of heat conduction to the tube walls and via thermal radiation); m is the mass flow rate; l is the heater location; and L is the tube length. Eq. (11) utilizes the balance of thermoacoustic power input and acoustic losses. The stability boundaries, calculated using Eq. (11), are shown in Fig. 8 by dashed lines. A deviation between the two theories is observed. It demonstrates that variation of the temperature field, affecting acoustic mode properties, is an important factor in determining the system stability. Uniform temperature approximation moves stability boundary mainly downward, i.e., instability is observed at lower power. This characteristic is explained by the fact that in a non-uniform temperature field, the mode shapes are distorted from the ideal sinusoidal forms, and consequently, the heater appears to be located at points which do not coincide with the most favorable locations to initiate instability. The agreement of the constant temperature model with experimental data is generally less accurate, though the behavior of the stability boundary is captured. Note that we still utilize the results of a complete heat transfer analysis; if a simplified version of thermal modelling is applied, the prediction of acoustic instability will degrade further.

The frequencies of the acoustic modes on the verge of transition to instability are also of interest for model validation and practical purposes. The calculated values of these critical frequencies are shown in Fig. 9. Experimentally recorded dominant frequencies, given in Fig. 9, correspond to the excited states recorded after transition to instability. The data scatter is due partly to unequal locations of these states from the stability boundary. Both experimental and theoretical values manifest the same tendency. Precise comparison of the measured frequencies and the frequencies found by the linear model is not appropriate and is not a purpose of this study, since the measured frequencies correspond to the excited steady states, which are significantly affected by non-linear effects and by the modified temperature field when the acoustic velocity is comparable with the mean flow velocity.

6. Concluding remarks

The work reported in this paper was carried out with two primary intentions: (1) to obtain accurate data for the boundary of stability for acoustic oscillations in a Rijke tube; and (2) to determine how accurately the observed results could be reproduced by analysis of the linear behavior of small amplitude oscillations.

An unexpected experimental result requiring explanation was the observation of apparent hysteresis in the stability boundary at high mass flow rate. This behavior, not previously reported, could be found relatively easily in the apparatus used in this work because with an electrically heated tube, the mass flow rate can be controlled independently of the power input: combustion-driven Rijke tubes do not allow that flexibility.

Owing to the very low Mach number of the mean flow, interactions between the mean flow and the oscillating field can be ignored in the acoustic analysis. Hence the influence of the average flow

appears only at the heater. However, to obtain satisfactory theoretical results, it is essential to account for the axial variations of the temperature, measured as a part of the experimental work. Thus, a thorough thermal analysis must be carried out to determine the mean temperature; only in that way is the theoretical prediction of the stability boundary entirely independent of the experimental results.

The computed results are in quite good agreement with the stability boundaries observed. A larger error in the predicted stability boundary is introduced if the temperature is assumed to be uniform, although the general behavior is captured (Fig. 8). Errors at the high and low flow rates may be due to inaccurate representation of the transfer function of the heater. A linear model is unable to describe a hysteresis effect. Modified temperature field and non-linearity of the transfer function in the presence of comparable mean and oscillatory velocities are probably the main reasons for hysteresis.

These results suggest that the approach taken here should be applicable to assessing the stability of motion in other thermal devices, such as combustion-driven Rijke tubes, combustors, and thermoacustic engines, if the Mach number of the average flow is small. Two generally important points must be emphasized: (1) non-uniformities of the temperature field significantly affect the stability boundaries; (2) as always in the case for unsteady behavior in combustion systems, the greatest unknown is the interaction (feedback) between the unsteady motion and the source of energy. The behavior of the Rijke tube observed and explained in this work clearly confirms the points.

Acknowledgements

Mr. Dylan Hixon, formerly a graduate student at Caltech, designed and constructed the original version of the apparatus used in this work. The authors wish to thank Dr. Winston Pun and Mr. Steve Palm for the help with recent improvements of the apparatus, instrumentation, and data processing. This work was supported in part by the California Institute of Technology, partly by the Caltech Multidisciplinary University Research Initiative under Grant No. N00014-95-1-1338 (Dr. Judah Goldwasser, Program Manager), partly by the Department of Energy Advanced Gas Turbine Systems Research (AGTSR) Program under Subcontract No. 98-02-SR072 (Dr. Daniel Fant & Dr. Larry Golan, Program Managers), and partly by the Air Force Office of Scientific Research (AFOSR) under Grant No. F49620-99-1-0118 (Dr. Mitat Birkan, Program Manager).

Appendix A. Explanation of sound apperance

This appendix shows how a simple explanation of Rijke oscillations can be obtained using Rayleigh's criterion in the form of Eq. (1). The open-ended Rijke tube of length L with a concentrated air-permeable heat source, located at a distance l from the upstream tube end, is given in Fig. 10. The mean flow direction coincides with axis x. Only longitudinal flow fluctuations are considered. According to Rayleigh's criterion, expressed in the form of Eq. (1), the amount of energy transformed from the heat addition to the system acoustics during cycle

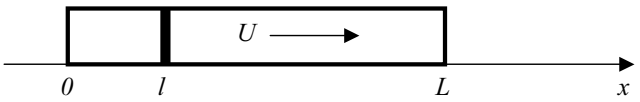

Fig. 10. One-dimensional Rijke tube with concentrated heat source.

period T is

$$\Delta E \sim \int_0^L \mathrm{d}x \int_0^T p' \dot{Q}' \,\mathrm{d}t, \tag{A.1}$$

where p' and $\dot{Q}'$ are fluctuations of pressure and heat release. If a flow velocity contains a small fluctuating component u', then unsteady component of the convective heat transfer rate $\dot{Q}'$ from a concentrated heat source can be expressed as follows:

$$\frac{\dot{Q}'(x,t)}{\dot{Q}_0} \sim \frac{u'(x,t-\tau)}{u_0}\,\delta(x-l). \tag{A.2}$$

where u_0 and $\dot{Q}_0$ are the mean flow velocity and the mean heat transfer rate; time delay τ is due to the thermal inertia, and δ is the delta function. Since both u_0 and $\dot{Q}_0$ are positive, we can write

$$\dot{Q}'(x,t) \sim u'(x,t-\tau)\delta(x-l). \tag{A.3}$$

Consider flow disturbances through eigen acoustic modes. Assume that the effects of unsteady heat addition and acoustic losses (due to boundary layer and radiation from open tube ends) are small enough for velocity and pressure perturbation amplitudes to vary little from cycle to cycle, and neglect by temperature variation along the tube; then the fluctuations in the nth acoustic mode are

$$u_n' \sim \cos(\omega_n t)\cos(k_n x), \quad p_n' \sim \sin(\omega_n t)\sin(k_n x), \tag{A.4}$$

where $\omega_n = \pi a n/L$; $k_n = \pi n/L$, and a is the speed of sound. Substituting Eqs. (A.3) and (A.4) into Eq. (A.1) and integrating over a chamber volume and a cycle period, we find that the energy input into the nth harmonic is

$$\Delta E_n \sim \sin\left(\frac{2\pi n l}{L}\right)\sin\left(\frac{\pi n a \tau_n}{L}\right). \tag{A.5}$$

The time delay τ_n is smaller than a half of period in commonly used Rijke tubes; hence the sign of thermal-acoustic energy transformation is determined by the first multiplier in Eq. (A.5). Only the lowest modes can be responsible for excitation, since acoustic losses grow fast with frequency increase. The conditions for a heater location, corresponding to the encouragement of the first two mode instabilities, are the following:

$$\Delta E_1 > 0 \quad \text{when } 0 < l < L/2, \quad \Delta E_2 > 0 \quad \text{when } 0 < l < L/4 \text{ or } L/2 < l < 3L/4. \tag{A.6}$$

This is in accordance with previous and the current experimental and theoretical results, for instance, in a vertical Rijke tube the self-excited oscillations with a fundamental frequency appear only when a gauze is located in the lower (upstream) half of the tube. The heater position in the first quarter of the tube may lead to excitation of both the two lowest modes; in order to

distinguish system instability induced by the second mode, a more favorable location for the heater is in the third quarter from the upstream tube end.

References

[1] F.E.C. Culick, V. Yang, Prediction of the stability of unsteady motions in solid-propellant rocket motors, Progress in Astronautics and Aeronautics 143 (1992) 719–779.
[2] T. Lieuwen, H. Torres, C. Johnson, B.T. Zinn, A mechanism of combustion instability in lean premixed gas turbine combustors, Journal of Engineering for Gas Turbines and Power 123 (2000) 1182–1189.
[3] G.W. Swift, Thermoacoustic engines, Journal of the Acoustical Society of America 84 (1988) 1145–1180.
[4] J.W.S. Rayleigh, The Theory of Sound, Dover Publications, New York, 1945.
[5] F.E.C. Culick, Nonlinear behavior of acoustic waves in combustion chambers. Parts I and II, Acta Astronautica 3 (1976) 714–757.
[6] P.L. Rijke, Philosophical Magazine 17 (1859) 419.
[7] R.L. Raun, M.W. Beckstead, J.C. Finlinson, K.P. Brooks, A review of Rijke tubes, Rijke burners and related devices, Progress in Energy and Combustion Science 19 (1993) 313–364.
[8] I.Y. Marone, A.A. Tarakanovskii, Investigation of sound generation in a Rijke tube, Soviet Physics—Acoustics 12 (1967) 261–263.
[9] Y. Katto, A. Sajiki, Onset of oscillation of a gas-column in a tube due to the existence of heat-conduction field, Bulletin of the Japanese Society of Mechanical Engineers 20 (1977) 1161–1168.
[10] H. Madarame, Thermally induced acoustic oscillations in a pipe, Bulletin of the Japanese Society of Mechanical Engineers 24 (1981) 1626–1633.
[11] J.C. Finlinson, M.A. Nelson, M.W. Beckstead, Characterization of a modified Rijke burner for measurement of distributed combustion, 24th JANNAF Combustion Meeting, Vol. 1, 1987, pp. 13–25.
[12] R.L. Raun, M.W. Beckstead, A numerical model for temperature gradient and particle effects on Rijke burner oscillations, Combustion and Flame 94 (1993) 1–24.
[13] H.J. Merk, Analysis of heat-driven oscillations of gas flows, Applied Scientific Research A 6 (1957) 402–420.
[14] B.J. Bayly, Heat transfer from a cylinder in a time-dependent cross flow at low Peclet number, The Physics of Fluids 28 (1985) 3451–3456.
[15] C. Nicoli, P. Pelce, One-dimensional model for the Rijke tube, Journal of Fluid Mechanics 202 (1989) 83–96.
[16] Y.-P. Kwon, B.-H. Lee, Stability of the Rijke thermoacoustic oscillation, Journal of the Acoustical Society of America 78 (1985) 1414–1420.
[17] K.I. Matveev, F.E.C. Culick, Experimental and mathematical modeling of thermoacoustic instabilities in a Rijke tube, 40th Aerospace Sciences Meeting and Exhibit, Reno NV AIAA paper 2002-1013, 2002.
[18] W. Pun, Measurements of Thermo-Acoustic Coupling, Ph.D. Thesis, Institute of Technology, California, 2001.
[19] R.M. Murray, Sparrow Reference Manual, California Institute of Technology, 1995.
[20] M.S. Howe, Acoustics of Fluid–Structure Interactions, Cambridge University Press, Cambridge, 1998.
[21] N.S. Dickey, A. Selamet, J.M. Novak, The effect of high-amplitude sound on the attenuation of perforated tube silencers, Journal of the Acoustical Society of America 108 (2000) 1068–1081.
[22] H. Levine, J. Schwinger, On the radiation of sound from an unflanged circular pipe, Physical Review Letters 73 (1948) 383–406.
[23] S.N. Gurbatov, O.V. Rudenko, Acoustics in Problems, Nauka, Moscow, 1996.
[24] U. Ingard, On the theory and design of acoustic resonators, Journal of the Acoustical Society of America 25 (1953) 1037–1061.
[25] V.O. Knudsen, C.M. Harris, Acoustical Designing in Architecture, Wiley, New York, 1950.
[26] M.A. Heckl, Non-linear acoustic effects in the Rijke tube, Acustica 72 (1990) 63–71.
[27] K.I. Matveev, F.E.C. Culick, On the nonlinear characteristics of a Rijke tube, Ninth International Congress on Sound and Vibration, Orlando, FL, 2002.